Surface & Coatings Technology 206 (2011) 770–774

Contents lists available at ScienceDirect

Surface & Coatings Technology

journal homepage: www.elsevier.com/locate/surfcoat

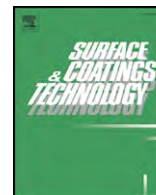

High-energy heavy ion beam annealing effect on ion beam synthesis of silicon carbide

J. Khamsuwan [a], S. Intarasiri [b], K. Kirkby [c], C. Jeynes [c], P.K. Chu [d], T. Kamwanna [e], L.D. Yu [a,e,*]

[a] Department of Physics and Materials Science, Faculty of Science, Chiang Mai University, Chiang Mai 50200, Thailand
[b] Science and Technology Research Institute, Chiang Mai University, Chiang Mai 50200, Thailand
[c] Surrey Ion Beam Centre, University of Surrey, Guildford, Surrey, GU2 7XH, UK
[d] Department of Physics and Materials Science, City University of Hong Kong, Tat Chee Avenue, Kowloon, Hong Kong, China
[e] Thailand Center of Excellence in Physics, Commission on Higher Education, 328 Si Ayutthaya Road, Bangkok 10400, Thailand

A R T I C L E I N F O

Available online 20 April 2011

Keywords:
High-energy heavy ion beam annealing
Silicon carbide (SiC)
Ion beam synthesis (IBS)
Crystallization

A B S T R A C T

Silicon carbide (SiC) is a superior material potentially replacing conventional silicon for high-power and high-frequency microelectronic applications. Ion beam synthesis (IBS) is a novel technique to produce large-area, high-quality and ready-to-use SiC crystals. The technique uses high-fluence carbon ion implantation in silicon wafers at elevated temperatures, followed by high-energy heavy ion beam annealing. This work focuses on studying effects from the ion beam annealing on crystallization of SiC from implanted carbon and matrix silicon. In the ion beam annealing experiments, heavy ion beams of iodine and xenon, the neighbors in the periodic table, with different energies to different fluences, I ions at 10, 20, and 30 MeV with 1–5×10^{12} ions/cm^2, while Xe ions at 4 MeV with 5×10^{13} and 1×10^{14} ions/cm^2, bombarded C-ion in implanted Si at elevated temperatures. X-ray diffraction, Raman scattering, infrared spectroscopy were used to characterize the formation of SiC. Non-Rutherford backscattering and Rutherford backscattering spectrometry were used to analyze changes in the carbon depth profiles. The results from this study were compared with those previously reported in similar studies. The comparison showed that ion beam annealing could indeed induce crystallization of SiC, mainly depending on the single ion energy but not on the deposited areal density of the ion beam energy (the product of the ion energy and the fluence). The results demonstrate from an aspect that the electronic stopping plays the key role in the annealing.

© 2011 Elsevier B.V. All rights reserved.

1. Introduction

Wide-band gap semiconductor materials, like silicon carbide (SiC), have much attracted microelectronic applications, owing to their excellent properties for devices operating under extreme conditions such as high temperature, high breakdown field, high saturation velocity, and inertness [1–4]. However, growth of SiC of high purity and good crystalline quality is not easy, but ion implantation is a recently developed technique to synthesize high-quality crystalline SiC. Ion beam synthesis (IBS) is a powerful tool of synthesizing novel materials. In conventional IBS, high-fluence ion implantation is employed to change the chemical composition in the near surface region of a substrate, followed by thermal annealing which is used for recovering the radiation induced defects and recrystallizing the materials. The most simple and traditional annealing is furnace annealing in high temperature ranging from 800 to 1200 °C [5–9]. Ion beam annealing used in the present study is based on the concept of ion beam induction of recrystallization. The technique uses MeV high-energy heavy ion beams to bombard material. Tremendous energy deposition from electronic stopping in the ion implantation process can result in the recrystallization of amorphous structures. Advantages of this technique include low temperature, short processing time, and localized treatment [10–12]. In this work, we focus on the formation of SiC using high-fluence carbon ion implantation in Si wafer and subsequent high-energy heavy ion beam annealing.

2. Experimental

Two-inch (100) p-type silicon wafers were used as the substrate. The Si wafers were first implanted with 90-keV or 40-keV carbon ions to a fluence of 6.5×10^{17} ions/cm^2 at an elevated temperature of 400 °C. After implantation, the silicon wafers were treated by two types of heavy ion beam annealing, one with lower energy but higher fluence xenon ions and the other with higher energy but lower fluence iodine, both of which are neighbors in the periodic table. The Xe-ion implantation was performed with a 2-MV Van De Graff Ion Accelerator at the Surrey Ion Beam Center, University of Surrey. The sample was irradiated by 4-MeV $^{131}Xe^{2+}$ ions to fluences of 5×10^{13} and 1×10^{14} ions/cm^2 at a target sample temperature of 500 °C. The Xe-ion bombardment was operated

* Corresponding author at: Department of Physics and Materials Science, Faculty of Science, Chiang Mai University, Chiang Mai 50200, Thailand. Tel.: +66 53 943379; fax: +66 53 222776.
E-mail address: yuld@fnrf.science.cmu.ac.th (L.D. Yu).

0257-8972/$ – see front matter © 2011 Elsevier B.V. All rights reserved.
doi:10.1016/j.surfcoat.2011.04.058

in different areas on the 90-keV C-ion implanted sample as shown in Fig. 1. For a comparison, multiply charged 10-, 20- and 30-MeV ^{127}I-ion beams to fluences of $1–5 \times 10^{12}$ ions/cm^2 were used for heavy ion beam annealing of the 40-keV C-ion implanted Si sample at various elevated temperatures at the Royal Institute of Technology in Sweden [12].

After ion beam annealing, the Si wafers were cut into 1×1-cm^2 square pieces for characterization at Chiang Mai University (CMU) and Hong Kong City University. Observation of the formation of SiC was carried out using both Infrared (IR) spectroscopy and Raman measurement. The IR spectra were obtained using a Perkin Elmer Fourier-transform infrared spectrometer in the range of 400–1500 cm^{-1} with a resolution of 4 cm^{-1}. The Raman scattering measurement was carried out using Renishaw 2000 with argon laser excitation at 514 nm in backscattering configuration. The crystalline structure of the SiC layer of the as-implanted and annealed samples was characterized using X-ray diffraction (XRD). The diffraction patterns were recorded in a Philips X'Pert system using Cu $K\alpha$ radiation (wavelength = 1.54 Å) at 40 kV, 30 mA and step size of 0.05°. Elastic (non-Rutherford) backscattering (EBS) and Rutherford backscattering spectrometry (RBS) analyses were performed for carbon depth profile information before (at Surrey) and after ion beam annealing (at Chiang Mai), respectively.

3. Results and discussion

Ion beam analysis was carried out to determine whether ion beam annealing had any effect on the carbon concentration depth profile. Fig. 2 displays the C-ion depth profiles extracted from the EBS and RBS spectra measured before and after Xe-ion beam annealing. The extraction of the real C-ion profiles from EBS and RBS spectra was performed using both DataFurnace code [13] and a self-developed software [14]. In general, the measured C-ion depth profiles reasonably agree with the SRIM-simulated one in basic parameters such as the range, range straggling and maximum concentration. A small profile shift is observed due to the ion beam annealing. The C profile after the lower fluence Xe-ion beam annealing has a very slight, almost negligible, shift to the surface side compared with that before the annealing. The C profile after the higher fluence ion beam annealing has a more noticeable shift and a slight decrease in the concentration as well. This phenomenon may imply an effect of heat absorption of the target from the ion beam annealing to cause loss of carbon probably due to formation of hydrocarbon [14] which eases the evaporation. Comparing this result with that from thermal annealing which caused no change in the carbon profiles [14], we can realize that the high-energy heavy ion beam bombardment is more effective in annealing than the thermal techniques.

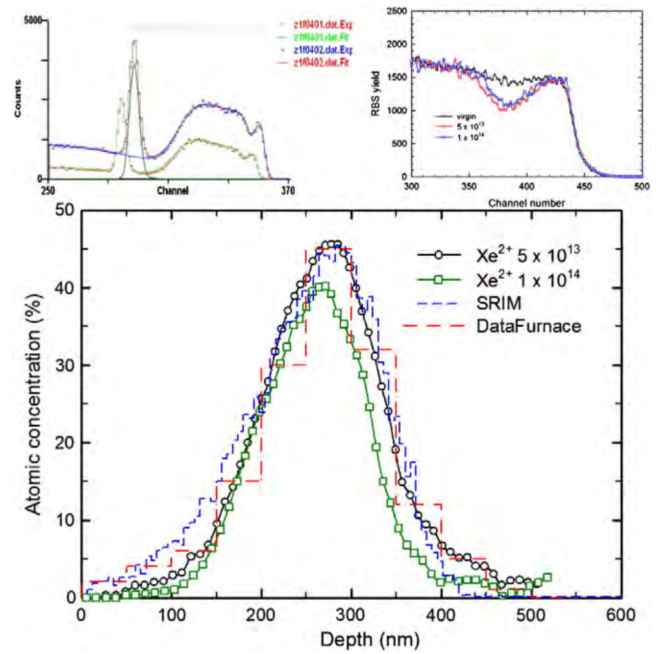

Fig. 2. Depth distributions of atomic concentration of C ions implanted in Si before and after ion beam annealing treated with Xe^{2+} analyzed by EBS, RBS and SRIM simulation. The SRIM-simulated and DataFurnace-calculated profiles are without ion beam annealing. The insets above the figure of the C-ion depth distribution are the original spectra of EBS (left) and RBS (right).

The ion beam annealing effect on recrystallization was examined. Fig. 3 shows the X-ray diffraction pattern of the carbon as-implanted Si and the sample subsequently ion beam annealed with 4-MeV $^{131}Xe^{2+}$ ions to fluences of 5×10^{13} and 1×10^{14} ions/cm^2. Three peaks are seen at $2\theta = 41.4°$, 89.2° and 69.4° corresponding to β-SiC (200), (400) and Si (400), respectively [15–17]. For the as-implanted sample, the peak intensities are all weak or even unobservable, while those of the Xe-irradiated samples are strong. The noticeable enhancement in the intensity of the Si peak indicates a strong effect of the heavy ion beam annealing on the recrystallization of the Si substrate. The significant increase in the intensities of the SiC peaks demonstrate that the Xe-ion beam annealing plays a critical role in producing the silicon carbide phase of the 3 C polytype, the same as I-ion beam

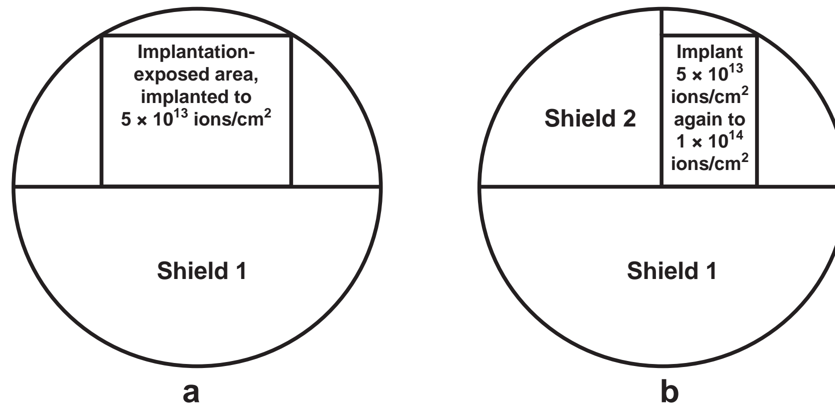

Fig. 1. The Si wafer with shielded areas for Xe-irradiation. (a) The area exposed for the first Xe-bombarded to a fluence of 5×10^{13} ions/cm^2. (b) The area exposed for the second Xe-bombarded to a final fluence of 1×10^{14} ions/cm^2. The area with "Shield 1" was never exposed to the ion beam during the irradiation and was used as the as-implanted area.

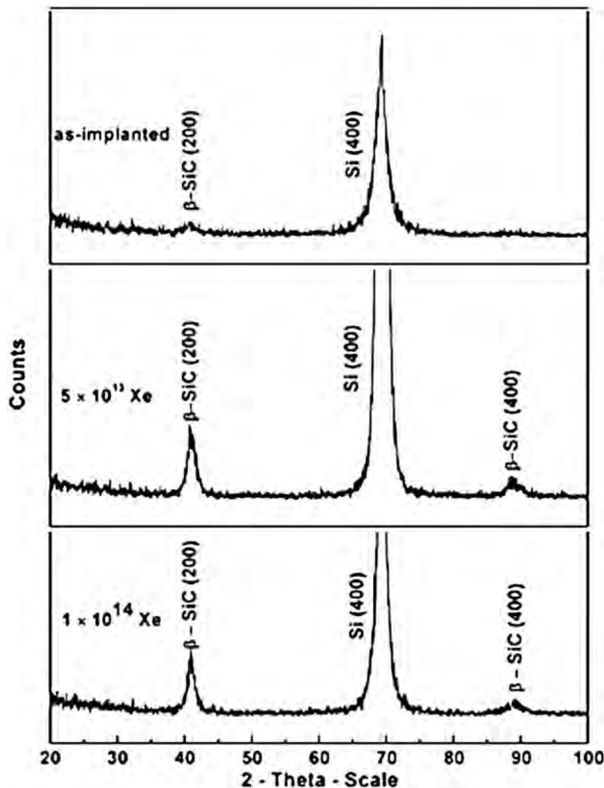

Fig. 3. The X-ray diffraction pattern of the carbon as-implanted Si and the sample subsequently ion beam annealed with 4-MeV $^{131}Xe^{2+}$ ions to fluences of 5×10^{13} and 1×10^{14} ions/cm^2.

irradiation induced SiC layer [12]. The grain size of the polycrystalline SiC was calculated from Scherrer formula [18]

$$t = \frac{K\lambda}{B\ \cos\left(\frac{2\theta_B}{2}\right)}, \qquad (1)$$

where t is the grain size, λ is the wavelength of the radiation (1.54 Å), θ_B is the angle of the considered Bragg reflection, B is FWHM of the peak and K is a constant (0.89). The mean grain sizes of β-SiC are then 8.88 nm (400) and 5.24 nm (200), respectively, after the Xe-ion beam annealing, but about 4 nm for the as-implanted case. This shows that the high-energy heavy ion beam indeed anneals the crystalline structure.

The IR transmittance spectra of different Xe-irradiated areas on the C-ion implanted Si wafer substrate are shown in Fig. 4. An unimplanted silicon wafer was used to measure the background signal which had been subtracted from the spectra. A peak located at a wavenumber of ~796 cm^{-1} is obviously seen in all the spectra, and it is corresponding to the transversal optical (TO) phonon absorption of crystalline β-SiC [13,19–21]. For the as-implanted area, a small broad bump is present at about 750 cm^{-1} of the spectrum, and it is related to the presence of an amorphous SiC in the implanted layer [13,21]. After bombardment with Xe^{2+} beam to both fluences, the small bump at 750 cm^{-1} disappears and at the same time the Lorentzian band at 796 cm^{-1} significantly becomes sharper and stronger. The absorption in the ion beam annealing case due to the formation of β-SiC increases by more than two times compared with the absorption of the as-implanted case. These facts clearly show that the heavy ion beam annealing crystallizes the SiC. The IR spectra indicate that ion beam annealing even using a few MeV heavy Xe-ion beam is able to induce the formation of crystalline SiC. For higher-energy heavy I-ion beam

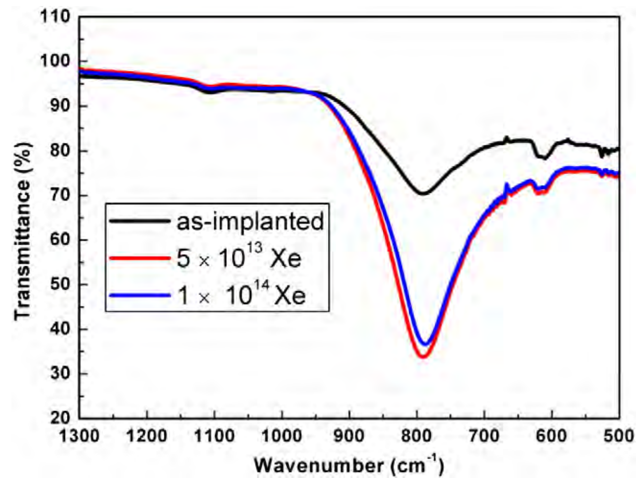

Fig. 4. IR transmittance spectra from the Xe-ion beam annealed samples, compared with that from the as-implanted sample.

annealing, the clear evidence of the induction of SiC formation has been reported elsewhere [21].

While the IR results show clear evidence of SiC formation induced by the heavy ion beam annealing, Raman measurement normally provides comparatively weak information. Nevertheless, Raman measurement results are still displayed here, as shown in Fig. 5, for some discussion. This analysis was operated in a range between 200 and 2000 cm^{-1}. For the as-implanted area, the spectrum shows a peak at 520 cm^{-1} corresponding to the longitudinal optical (LO) phonon mode of absorption of the crystalline Si [22] and the Si second-order peak at 970 cm^{-1}. In all cases, while the peaks at 520 cm^{-1} are still clear, the peaks at 970 cm^{-1} become less prominent in the Xe-irradiated areas than in the as-implanted area. This phenomenon may imply that the silicon becoming somehow slightly amorphized by the heavy ion bombardment. In the Raman spectra of the high-fluence ion irradiated area, although Raman scattering is a weak interaction between photons and phonons and thus sometimes comparatively not very sensitive, a small bump appears very near to 800 cm^{-1}. This indicates the formation of 3C-SiC (the TO mode of 3C-SiC at ~796 cm^{-1}) [12,13,23]. From this it may be assumed that heavy ion beam annealing induction of crystallization of SiC depends on the deposited heavy-ion energy. The higher fluence deposits more energy, and when the deposited energy is enough, the crystallization of SiC can occur. However, compared with the result of heavy ion beam annealing using higher energy but much lower fluence I-ion beam [12] (thus less deposited total areal ion energy, which is defined as the product of ion energy and fluence), I-irradiation produced more pronounced evidence in Raman spectrum for the crystallization of SiC as seen the bump around 796 cm^{-1} (Fig. 5b). In I-irradiation, the sample temperature during the ion beam annealing was 80, 400 and 800 °C, respectively. The results demonstrated that the Raman spectral peak heights had no significant difference between 400 °C and 800 °C. It can then be inferred that the Raman spectral features for I-irradiation would be similar if the target temperature was 500 °C, which was the case of Xe-bombarded. This implies that the ion energy is dominant in heavy ion beam annealing.

To understand the mechanisms involved in the high-energy heavy ion beam annealing induction of crystallization of SiC, a comparison in energy loss among several similar experiments of C-ion implanted Si was made as shown in Table 1. In the examples, the conditions of C-ion implantation in Si are similar. The first two cases are from our work, while the third is from the work of [9], in which no SiC crystallization effect was observed. Both of the first two high-energy heavy ion beam bombardments were operated at elevated temperatures, which had no noticeable difference in the effect on the

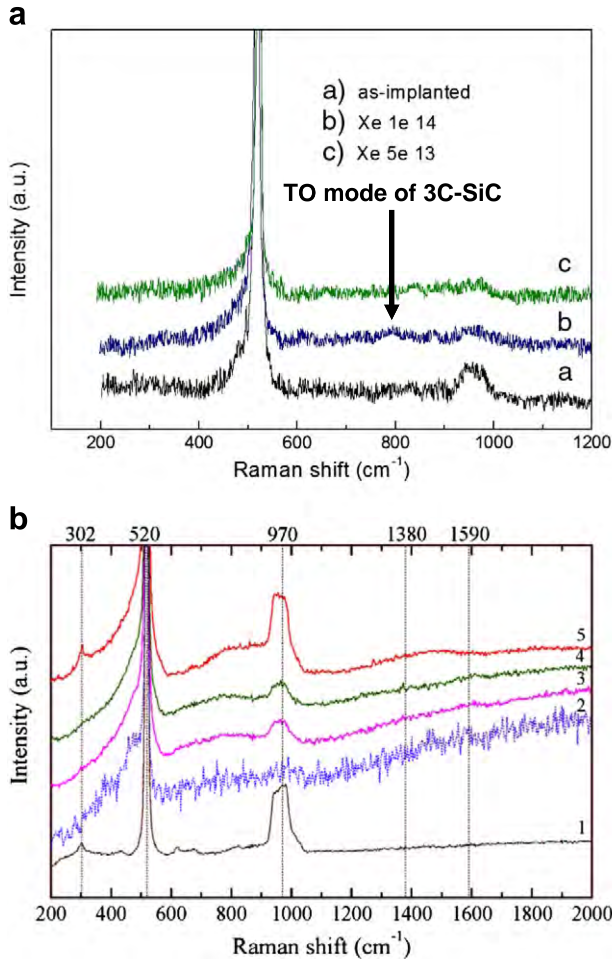

Fig. 5. Raman spectra from (a) Xe-ion beam and (b) I-ion beam annealed samples compared with those from the as-implanted samples. In (b), spectrum 1: Si substrate, 2: as-implanted, 3: 20-MeV I-ion beam annealing, 4: 30-MeV I-ion beam annealing, and 5: thermal annealing at 1000 °C.

formation of SiC, as mentioned above. In these two cases, it is seen that either in the entire heavy ion traveling region or in the C-ion implanted region, the electronic stopping of the 20-MeV I-ion beam is more dominant than that of the 4-MeV Xe-ion beam, while the nuclear stopping of the former is much less important than that of the latter. If the areal electronic-stopping-deposited energy densities, calculated by the energy loss due to the electronic stopping in the SiC region multiplied by the ion fluence, are compared, it is found that the areal energy density of the Xe-ion beam case is about 40 times than that of the I-ion case. However, the experimental results showed that the I-ion beam was more effective in the crystallization of SiC. This fact may indicate that the ion energy plays a more significant role in the crystallization than the areal ion energy density, which reflects the total ion energy deposited in the implanted carbon region. But, in the case of the 100-MeV Ag-ion beam annealing, both the portion of the electronic stopping and the energy deposited due to the electronic stopping in the C-ion region are far more than those of the I-ion beam case. It would then be expected to induce more pronounced SiC crystallization but the fact is not. The reason is that in the Ag-ion beam annealing room temperature was used, whereas in our cases elevated temperature was applied, which could activate the mobility of atoms for nucleation. Although high-energy ion beam also deposits energy via the thermal spikes, the quenching time for a thermal spike to cool down or transfer energy is too short, some order of 10^{-13} s [24], for atoms to start nucleation. Therefore, the process of the high-energy heavy ion beam annealing of SiC can be suggested such that at an elevated temperature (which may be only about a few hundred degrees °C, not necessarily as high as that used in thermal annealing, e.g. more than 1000 °C), carbon atoms are thermally mobile to bind with silicon to nucleate SiC seeds. Simultaneously, each single swift heavy ion loses its large portion of the initial energy via the electronic stopping and deposits and transfers the energy via the electron–phonon interaction to the lattice and carbon atoms. This energy transfer that takes place around the single ion track should be effective enough for carbon and silicon atoms to overcome energy barriers between them and the SiC seed for the SiC grain to grow. Hence, the more the single ion energy is transferred, the higher the effect on the crystallization of SiC.

4. Conclusion

Crystalline β-SiC could be synthesized by low-energy C-ion implantation in Si wafers followed by subsequent high-energy heavy ion beam annealing instead of high-temperature thermal annealing. In the comparative study, Xe and I ions which had similar masses but different energy and fluences were used for ion beam annealing. Results showed that heavy ion beam annealing induced crystallization of SiC was dominated by the single ion energy but not on the total areal ion beam energy deposited in the C-ion implanted region. The results demonstrate that the electronic stopping plays a key role in annealing for crystallization of SiC. A successful ion beam annealing is proposed to be operated using higher energy and lower fluence of heavy ion beams combined with using a moderately elevated temperature.

Acknowledgements

The work was supported by The National Electronic and Computer Technology Center of Thailand, Thailand Research Fund, the International Atomic Energy Agency (IAEA) under the Coordinated Research Projects on Ion Beam Modification of Insulators, and Thailand Center of Excellence in Physics. J. K. wishes to thank the scholarship of the Plasma Laboratory, City University of Hong Kong.

Table 1

Comparisons in energy loss among three experiments on high-energy heavy ion beam annealing of C-ion-implanted Si based on SRIM simulations. The conditions of the 100-MeV Ag-ion beam annealing are taken from [9]. The ion range and the maximum C-ion depth, which is considered such that beyond this depth, the C concentration is negligible, are obtained from the simulation. S_e: electronic stopping. S_n: nuclear stopping. S: total stopping, i.e. $S = S_e + S_n$. ΔE_e: energy loss due to electronic stopping. N_n: number of collision events due to nuclear stopping. S_e, S_n, S, ΔE_e and N_n as well as S_e/S and S_n/S are all obtained from the simulation. (SiC): within the ion-implantation synthesized SiC region or the maximum C-ion depth. ΔE_e(SiC) and N_n(SiC) are estimated from the integrated area under the SRIM-simulated ionization energy loss curve and collision event curve in the (SiC) regions, respectively. dE_e(SiC): areal S_e-deposited energy density in the (SiC) region, calculated by $\Delta E_e(SiC) \times$ fluence.

High-energy heavy ion beam annealing conditions	Heavy ion range (μm)	Maximum C-ion depth (μm)	$\frac{S_e}{S}$ (%)	$\frac{S_n}{S}$ (%)	$\Delta E_e(SiC)$ (keV)	N_n(SiC) (number/ion)	dE_e(SiC) (keV/cm^2)
4-MeV Xe, 5×10^{13} ions/cm^2, 500 °C	1.49	0.42 (90-keV C-ion)	72	28	920	4800	4.6×10^{16}
20-MeV I, 1×10^{12} ions/cm^2 400 °C	6.21	0.23 (40-keV C-ion)	90	10	1080	800	1.1×10^{15}
100-MeV Ag, 5×10^{13} ions/cm^2, room temperature	15.7	0.27 (50 keV C-ion)	98	2	2808	160	1.4×10^{17}

References

[1] Z.C. Feng, S.C. Lien, J.H. Zhao, X.W. Sun, W. Lu, Thin Solid Films 516 (2008) 5217.
[2] Y.F. Chen, X.Z. Lui, X.W. Deng, Y.R. Li, Thin Solid Films 517 (2009) 2882.
[3] C.K. Chung, B.H. Wu, T.S. Chen, C.C. Peng, C.W. Lai, Thin Solid Films 517 (2009) 5867.
[4] H.X. Zhang, P.X. Feng, V. Makarov, B.R. Weiner, G. Morell, Mater. Res. Bull. 44 (2009) 184.
[5] Z.J. Zhang, K. Narumi, H. Naramoto, S. Yamamoto, A. Miyashita, J. Phys. D Appl. Phys. 32 (1999) 2236.
[6] K. Saravanan, B.K. Panigrahi, S. Amirthapandian, K.G.M. Nair, Nucl. Instrum. Meth. B 266 (2008) 1502.
[7] R.M.S.D. Reis, R.L. Maltez, H. Boudinov, Nucl. Instrum. Meth. B 267 (2009) 1281.
[8] B.G. Streetman, IEEE T. Nucl. Sci. NS-28 (2) (1981) 1742.
[9] Y.S. Katharria, F. Singh, P. Kumar, D. Kanjilal, Nucl. Instrum. Meth. B 254 (2007) 78.
[10] J.S. Williams, M.C. Ridgway, R.G. Elliman, J.A. Davies, S.T. Johnson, G.R. Palmer, Nucl. Instrum. Meth. B 55 (1991) 602.
[11] P.K. Sahoo, T. Som, D. Kanjilal, V.K. Kulkarni, Nucl. Instrum. Meth. B 240 (2005) 239.
[12] S. Intarasiri, L.D. Yu, S. Singkarat, A. Hallén, J. Lu, M. Ottosson, J. Jensen, G. Possnert, J. Appl. Phys. 101 (2007) 084311.
[13] N. P. Barradas, C. Jeynes, and R. P. Webb. Appl. Phys. Lett. 71 (1997) 291; Chris Jeynes, The IBA DataFurnace Homepage, http://www.ee.surrey.ac.uk/IBC/ndf/(2005)
[14] S. Intarasiri, T. Kamwanna, A. Hallén, L.D. Yu, M.S. Janson, C. Thongleum, G. Possnert, S. Singkarat, Nucl. Instrum. Meth. B 249 (2006) 859.
[15] J.H. Boo, K.S. Yu, M. Lee, Y. Kim, Appl. Phys. Lett. 66 (25) (1995) 3486.
[16] Z.J. Zhang, K. Narumi, H. Naramoto, S. Yamamoto, A. Miyashita, J. Phys. D Appl. Phys. 32 (1999) 2236.
[17] S.H. Jeong, D.C. Lim, H.-G. Jee, O.M. Moon, C.-K. Jung, J.S. Moon, S.K. Kim, S.-B. Lee, J.-H. Boo, J. Vac. Sci. Technol. B 22 (4) (2004) 2216.
[18] J.I. Langford, A.J.C. Wilson, J. Appl. Crystallogr. 11 (1978) 102.
[19] W. Wu, D.H. Chen, J.B. Xu, W.Y. Cheng, S.P. Wong, I.H. Wilson, R.W.M. Kwok, J. Vac. Sci. Technol. A 16 (3) (1998) 968.
[20] Y. Ito, T. Yamacuhi, A. Yamamoto, M. Sasase, S. Nishio, K. Yasuda, Y. Ishigami, Appl. Surf. Sci. 238 (2004) 159.
[21] S. Intarasiri, A. Hallén, J. Lu, J. Jensen, L.D. Yu, K. Bertilsson, M. Wolborski, S. Singkarat, G. Possnert, Appl. Surf. Sci. 253 (2007) 4836.
[22] Y.S. Katharria, S. Kumar, F. Singh, J.C. Pivin, D. Kanjilal, J. Phys. D Appl. Phys. 39 (2006) 3969.
[23] T. Zorba, D.I. Siapkas, C.C. Katsidis, Microelectron. Eng. 28 (1995) 229.
[24] M. Nastasi, J.W. Mayer, J.K. Hirvonen, Ion-solid Interactions: Fundamentals and Applications, Cambridge University Press, New York, 1996.